[4] S. T. Peng, T. Tamir, and H. L. Bertoni, "Theory of periodic dielectric waveguides," *IEEE Trans. Microwave Theory Tech.*, vol. MTT-23, pp. 123–133, Jan. 1975.
[5] J. E. Goell, "A circular-harmonic computer analysis of rectangular dielectric waveguides," *Bell Syst. Tech. J.*, vol. 48, pp. 2133–2160, Sept. 1969.
[6] M. Tsuji, S. Suhara, H. Shigesawa, and K. Takiyama, "Submillimeter guided-wave experiments with dielectric rib waveguides," *IEEE Trans. Microwave Theory Tech.*, vol. MTT-29, pp. 547–552, June 1981.
[7] T. Itoh, "Inverted strip dielectric waveguide for millimeter-wave integrated circuits," *IEEE Trans. Microwave Theory Tech.*, vol. MTT-24, pp. 821–827, Nov. 1976.
[8] R. Mittra, Y. Hou, and V. Jamnejad, "Analysis of open dielectric waveguides using mode-matching technique and variational methods," *IEEE Trans. Microwave Theory Tech.*, vol. MTT-28, pp. 36–43, Jan. 1980.
[9] S. M. Rao, E. Arvas, and T. K. Sarkar, "Combined field solution for TM scattering from multiple conducting and dielectric cylinders of arbitrary cross section," *IEEE Trans. Antennas Propagat.*, vol. AP-35, pp. 447–451, April 1987.
[10] E. Arvas and T. K. Sarkar, "RCS of two-dimensional structures consisting of both dielectrics and conductors of arbitrary cross section," *IEEE Trans. Antennas Propagat.*, vol. 37, pp. 546–554, May 1989.
[11] K. Umashankar, A. Taflove, and S. M. Rao, "Electromagnetic scattering by arbitrary shaped three-dimensional homogeneous lossy dielectric objects," *IEEE Trans. Antennas Propagat.*, vol. AP-34, pp. 758–766, June 1986.
[12] A. W. Glisson, "An integral equation for electromagnetic scattering from homogeneous dielectric bodies," *IEEE Trans. Antennas Propagat.*, vol. AP-32, pp. 173–175, Feb. 1984.
[13] G. W. Hohmann, "Three-dimensional induced polarization and electromagnetic modeling," *Geophys.*, vol. 40, pp. 309–324, Apr. 1975.
[14] M. J. Hagmann, O. P. Gandhi, and C. H. Durney, "Numerical calculation of electromagnetic energy deposition for a realistic model of man," *IEEE Trans. Microwave Theory Tech.*, vol. MTT-27, pp. 804–809, Sept. 1979.
[15] T. K. Sarkar, E. Arvas, and S. Ponnapalli, "Electromagnetic scattering from dielectric bodies," *IEEE Trans. Antennas Propagat.*, vol. 37, pp. 673–676, May 1989.
[16] D. H. Schaubert, D. R. Wilton, and A. W. Glisson, "A tetrahedral modeling method for electromagnetic scattering by arbitrarily shaped inhomogeneous dielectric bodies," *IEEE Trans. Antennas Propagat.*, vol. AP-32, pp. 77–85, Jan. 1984.
[17] M. F. Cátedra, E. Gago, and L. Nuño, "A numerical scheme to obtain the rcs of three-dimensional bodies of resonant size using the conjugate gradient method and the fast fourier transform," *IEEE Trans. Antennas Propagat.*, vol. 37, pp. 528–537, May 1989.
[18] R. F. Harrington and J. R. Mautz, "An impedance sheet approximation for thin dielectric shells," *IEEE Trans. Antennas Propagat.*, vol. AP-23, pp. 531–534, July 1975.
[19] J. H. Richmond, "A wire-grid model for scattering by conducting bodies," *IEEE Trans. Antennas Propagat.*, vol. AP-14, pp. 782–786, Nov. 1966.
[20] D. A. Hill and J. R. Wait, "Electromagnetic surface wave propagation over a bonded wire mesh," *IEEE Trans. Electromagn. Compat.*, vol. EMC-19, pp. 2–7, Feb. 1977.
[21] B. J. Rubin, "Full-wave analysis of waveguides involving finite-size dielectric regions," to be published in *1990 IEEE MTT-S Int. Microwave Symp. Dig.* (Dallas, TX), May 8–10, 1990.
[22] B. J. Rubin, "Electromagnetic approach for modeling high-performance computer modules," *IBM J. Res. Develop.*, to be published.
[23] B. J. Rubin, "Modeling arbitrarily shaped signal lines and discontinuities," *IEEE Trans. Microwave Theory Tech.*, vol. 37, pp. 1057–1060, June 1989.
[24] B. J. Rubin, "The propagation characteristics of signal lines in a mesh-plane environment," *IEEE Trans. Microwave Theory Tech.*, vol. MTT-32, pp. 522–531, May 1984.
[25] B. J. Rubin and H. L. Bertoni, "Waves guided by conductive strips above a periodically perforated ground plane," *IEEE Trans. Microwave Theory Tech.*, vol. MTT-31, pp. 541–549, July 1983.
[26] C. H. Chan and R. Mittra, "The propagation characteristics of signal lines embedded in a multilayered structure in the presence of a periodically perforated ground plane," *IEEE Trans. Microwave Theory Tech.*, vol. 36, pp. 968–975 June 1988.
[27] A. R. Djordjević and T. K. Sarkar, "A theorem on the moment methods," *IEEE Trans. Antennas Propagat*, vol. AP-35, pp. 353–355, Mar. 1987.
[28] J. R. Mautz and R. F. Harrington, "An *E*-field solution for a conducting surface small comparable to the wavelength," *IEEE Trans. Antennas Propagat.*, vol. AP-32, pp. 330–339, Apr. 1984.
[29] B. J. Rubin and S. Daijavad, "Radiation and scattering from structures involving finite-size dielectric regions," submitted to *IEEE Trans. Antennas Propagat.*

A Local Mesh Refinement Algorithm for the Time Domain–Finite Difference Method Using Maxwell's Curl Equations

IHN S. KIM, STUDENT MEMBER, IEEE, AND
WOLFGANG J. R. HOEFER, SENIOR MEMBER, IEEE

***Abstract*—In this paper we consider an efficient local mesh refinement algorithm subdividing a computational domain to resolve fine dimensions in a TD–FD space–time grid structure. At a discontinuous coarse–fine mesh interface, the boundary conditions for the tangential and normal field components are enforced for a smooth transition of highly nonuniform field quantities.**

I. Introduction

It is rather straightforward to model a region with smoothly varying field by using a uniform grid system of large mesh size. However, when the computational domain contains sharp discontinuities or objects, the fields become highly nonuniform in the vicinity of the discontinuities, and a mesh of very small mesh size must be employed. This requires a very extensive computational effort.

There are two ways to take into account the strong nonuniformity around a local discontinuity. The first is to use a mesh with gradually changing mesh size as it is currently employed in the TLM method. Such a procedure was introduced in the TD–FD method by Choi and Hoefer [1]. The problem with this method is that for a constant stability factor throughout the mesh, the time step Δt must always be varied in accordance with the local mesh size Δl.

In this paper, we propose an alternative approach, which was presented in more general form by Berger and Oliger [2] in 1984 for simple general hyperbolic partial differential equations. We have applied this approach specifically to Maxwell's two curl equations. In this approach we embed a locally uniform mesh of higher density into the larger mesh. The local uniformity of the mesh is important for keeping the same stability criterion during a simulation. This means that in the different subparts of the mesh, the ratio of Δt to Δl is kept the same. This has the advantage that in all subareas of the mesh exactly the same TD–FD algorithm can be employed.

Furthermore, Holland and Simpson [3] introduced the thin-strut formalism to include arbitrarily fine wires in their TD–FD code, THREDE, in 1981. Kunz and Simpson [4] also introduced an expansion approach to resolve locally fine objects. They first computed the field with a coarse mesh, thus obtaining the values of the tangential electric field at interfaces with a subsequently refined mesh area, which was analyzed in a second run.

In our approach, the coarse and the fine mesh regions are solved simultaneously, and the boundary conditions between the two regions are enforced to ensure a smooth transition of highly nonuniform field quantities. Furthermore, this scheme is recursive; that is, it can provide a finer and finer resolution if necessary.

Manuscript received September 5, 1989, revised January 15, 1990. This work was supported by the Natural Science and Engineering Research Council of Canada and by the Telecommunication Research Institute of Ontario.

The authors are with the Department of Electrical Engineering, University of Ottawa, 770 King Edward Ave., Ottawa, Ont., Canada K1N 6N5.

IEEE Log Number 9034900.

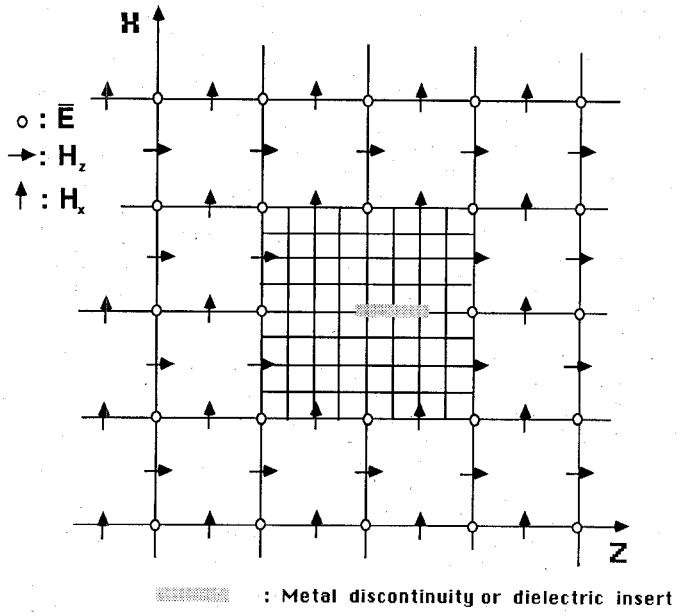

Fig. 1. The 1:4 local mesh refinement scheme in two space dimensions, and the field components allocated on the cell by Ampere's law.

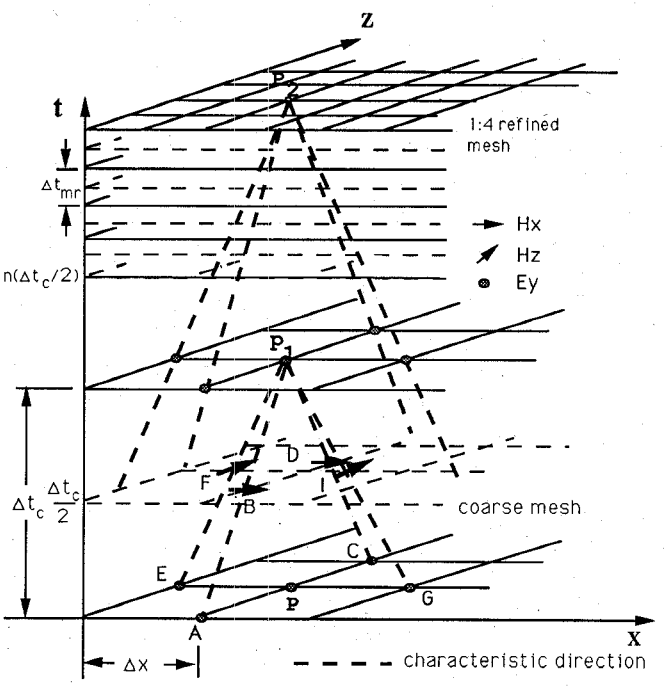

Fig. 2. Three-dimensional (x, z, t) diagram showing the leapfrog scheme following the lines of determination of Maxwell's two curl equations. The $\vec{E}$ fields are calculated at the points A, E, C, G, and P, and the $\vec{H}$ fields at the points B, F, D, and I for TE mode propagation.

The algorithm for this local mesh refinement scheme is presented in detail in Section II. To demonstrate the accuracy and the efficiency of our algorithm, we have modeled a thin metallic discontinuity in a rectangular waveguide and have compared the results with those obtained with a uniform mesh. This is done in Section III. Finally, we will discuss some limitations of the approach and conclude.

II. Mesh Refinement Algorithm

For ease of understanding, we introduce the mesh refinement algorithm for the two space dimensional case and assume TE mode propagation. In this case, the discretized Maxwell's equations are

$$H_x^{n+1/2}\left(i,k+\frac{1}{2}\right) = H_x^{n-1/2}\left(i,k+\frac{1}{2}\right) + \frac{c\Delta t}{Z_0\Delta z}\left[E_y^n(i,k+1) - E_y^n(i,k)\right] \quad (1a)$$

$$H_z^{n+1/2}\left(i+\frac{1}{2},k\right) = H_z^{n-1/2}\left(i+\frac{1}{2},k\right) - \frac{c\Delta t}{Z_0\Delta x}\left[E_y^n(i+1,k) - E_y^n(i,k)\right] \quad (1b)$$

$$E_y^{n+1}(i,k) = E_y^n(i,k) + \frac{Z_0 c\Delta t}{\Delta z}\left[H_x^{n+1/2}\left(i,k+\frac{1}{2}\right) - H_x^{n+1/2}\left(i,k-\frac{1}{2}\right)\right] - \frac{Z_0 c\Delta t}{\Delta x}\left[H_z^{n+1/2}\left(i+\frac{1}{2},k\right) - H_z^{n+1/2}\left(i-\frac{1}{2},k\right)\right] \quad (1c)$$

where indices (i, k) correspond to the Cartesian coordinates $(x, z,)$.

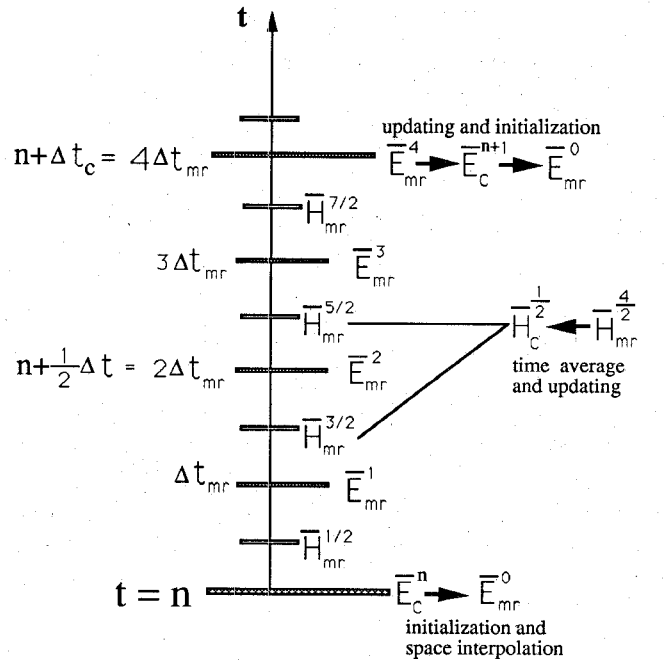

Fig. 3. The 1:4 mesh refinement scheme sequence along the time axis.

The computational cell for the TE mode and the definition of the field vector components in a cell are shown in Fig. 1. The fine mesh is denser than the coarse mesh by a factor of 4. Fig. 2 illustrates the leapfrog scheme which all previous authors have used, in three dimension (x, z, t), and shows the lines of determination for the discretized Maxwell equations (dotted lines). The propagation of the waves corresponding to the TD–FD

TABLE I
COMPARISON OF ACCURACY OF $|S_{11}|$ AND CPU TIME FOR THE THREE DIFFERENT MESH SCHEMES TO ANALYZE A 5-MIL-THICK AND 5-MIL-LONG METAL INSERT DISCONTINUITY IN WR-28 AT 27 GHz ON VAX-11/750

scheme	CPU sec	|S11|	Wavelength(m)	computational mesh size
uniform fine mesh	38998.74	0.856	0.01778	57 * 681
local refined mesh	537.68	0.834	0.01827	15 * 171 + 9 * 9
uniform coarse mesh	322.72	0.237	0.01524	15 * 171
	72.5 times faster		0.01777 theoretical result	

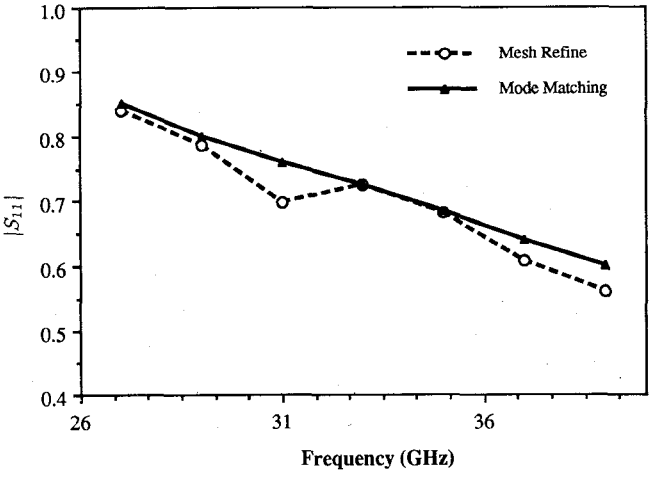

Fig. 4. $|S_{11}|$ comparison with the mode matching technique for the whole WR-28 operating frequency range.

solution should point in the direction of these lines of determination. As a first principle, these lines of determination should be continuous, even in the region with discontinuous mesh size. Second, field values calculated in the coarse and in the fine mesh region must satisfy the interface conditions at the boundaries between the two.

It is also recommended that the stability criteria remain the same in the coarse and in the fine mesh. In the case of a mesh ratio of 1 to 4, this means that the time increment in the fine mesh must be one fourth the time increment in the coarse mesh, as shown in Fig. 3. Note, however, that any integer mesh ratio may be chosen.

The main task in the mesh refinement algorithm for Maxwell's curl equations is to ensure continuity of fields across the interfaces between coarse and fine meshes. In the following we summarize the three steps which are schematically indicated in Fig. 3 along the time axis:

1) Initialize the field values at the coarse–fine mesh boundary by setting $E_c^n = E_{mr}^0$, $E_c^{n+1} = E_{mr}^4$. The superscript designates the time step, and the subscripts *mr* and *c* designate the refined and coarse mesh, respectively. Hence, the boundary values in the fine mesh are calculated by *initializing and interpolating* values in the coarse mesh. For example, for $1 \leqslant k \leqslant m-1$, E_{mr}^k is obtained by linear interpolation in time between E_c^n and E_c^{n+1}, or, equivalently, E_{mr}^0 and E_{mr}^4 on the time–space interface.

2) Obtain $\vec{H}_c^{n+1/2} = \vec{H}_{mr}^{4/2}$, and $\vec{E}_c^{n+1/2}$ by *time and space averaging* of $\vec{H}_{mr}^{5/2}$ and $\vec{H}_{mr}^{3/2}$ and *time averaging* of $\vec{E}_c^n$ and $\vec{E}_c^{n+1}$, respectively, since the field values of $\vec{H}_c^{n+1/2} = \vec{H}_{mr}^{4/2}$ and $\vec{E}_c^{n+1/2} = \vec{E}_{mr}^2$ are required to follow the lines of determination of Maxwell's two curl equations. Note that there are no $\vec{H}_{mr}^{4/2}$ and $\vec{E}_c^{n+1/2}$ on the boundaries of the space–time grid structure in the 1:4 ratio scheme at first.

3) Update field values by injecting the fine mesh solution values into the coarse mesh. Since a finer mesh is nested in a coarse mesh, the field values on the boundaries (interfaces) are *updated* every Δt_c, i.e., every $4\Delta t_{mr}$. The strongly nonuniform field behavior in the fine mesh region is transferred into the coarse mesh region by this step.

These three steps are performed at every coarse time step as shown in Fig. 3.

III. EXAMPLE

As an example, we have considered a local scattering problem in a standard rectangular waveguide (WR-28). A centered thin metal insert located in the E plane of the waveguide was considered. The object had a 5 mil thickness and a 5 mil length. To characterize the small object with a locally refined mesh, we injected a sinusoidal signal and processed it according to equations (1a)–(1c). Three different computations of the structure were performed, each with a different discretization scheme, namely a uniformly fine, a uniformly coarse, and a composite mesh with a 1:4 gridding ratio. The magnitude of S_{11} and the guided wavelength in the structure were computed in the three simulations. The accuracy of the latter has been verified by comparison with theoretical results for the guided wavelength. These values are shown in Table I. The CPU times for the three cases are also listed in the table. The mesh refinement scheme yielded very good results 70 times faster than the uniformly fine mesh, and represented a considerable improvement over the uniformly coarse mesh. In Fig. 4, $|S_{11}|$ obtained for the whole operating frequency range of WR-28 waveguide is compared with the result obtained with the mode matching technique for the same discontinuity above.

IV. CONCLUSIONS

A mesh refinement scheme for the standard TD–FD method has been presented. The results are promising. However, there are two problems that require caution when implementing the local mesh refinement algorithm [5]. First, the abrupt change of the mesh size invariably causes spurious reflections. These can be reduced by using a proper interpolating scheme conformal with the behavior of the solution. Second, any wave which is poorly resolved in a coarse mesh will change phase velocity when passing into a fine mesh. If this wave later passes from the fine mesh back into the coarse mesh, a serious interaction can result with that part of the wave which remained in the coarse mesh. To minimize this velocity error, care must be taken to ensure that the size of the coarse mesh is still much smaller than the shortest wavelength under study.

REFERENCES

[1] D. Choi and W. J. R. Hoefer, "A graded mesh FD–TD algorithm for eigenvalue problems," in *Proc. 17th European Microwave Conf.*, 1987, pp. 413–417.

[2] M. J. Berger and J. R. Oliger, "Adaptive mesh refinement for hyperbolic partial differential equation," *J. Comput. Phys.*, vol. 53, pp. 484–512, 1984.
[3] R. Holland and L. Simpson, "Finite difference analysis of EMP coupling to thin struts and wires," *IEEE Trans. Electromagn. Compat.*, vol. EMC-23, pp. 88–97, May 1981.
[4] K. S. Kunz and L. Simpson, "A technique for increasing the resolution of finite-difference solution of the Maxwell equation," *IEEE Trans. Electromagn. Compat.* vol. EMC-23, pp. 419–422, Nov. 1981.
[5] G. Browning, H-O. Kreiss, and J. R. Oliger, "Mesh refinement," *Math. Comput.*, vol. 27, no. 121, pp. 29–39, Jan. 1973.

Frequency-Domain Bivariate Generalized Power Series Analysis of Nonlinear Analog Circuits

PHILIP J. LUNSFORD II, STUDENT MEMBER, IEEE,
GEORGE W. RHYNE, MEMBER, IEEE, AND
MICHAEL B. STEER, MEMBER, IEEE

Abstract—**Bivariate generalized power series analysis is introduced for the analysis and behavioral modeling of nonlinear analog circuits and systems. It can be used to model analog subsystems and is compatible with circuit simulation. Thus full circuits and behaviorally modeled analog subcircuits can be simulated together in an analog circuit/system simulator. The entire analysis is performed in the frequency domain, and arbitrary nonlinear circuits and any number of noncommensurable input frequencies can be handled. A diode ring demodulator is analyzed as an example.**

I. Introduction

The simulation of complex analog circuits using harmonic balance and spectral balance techniques has developed rapidly in recent years. The analysis of nonlinear analog systems using behavioral modeling of nonlinear subsystems is less advanced, with Volterra series system analysis being the dominant method [1]. This technique, however, is limited to mildly nonlinear systems.

In this paper we present a frequency-domain modeling method that is an extension of the generalized power series analysis (GPSA), introduced by Steer and Khan [2]. GPSA is a frequency-domain simulation technique based on power series that, in general, can contain complex coefficients. However, GPSA can only be used with elements or systems having a single voltage or current controlling excitation. The bivariate GPSA introduced here can be used with elements or subsystems that have two controlling quantities and is more general than the power series method proposed by Narhi [3].

As an example, we present a behavioral model for a diode ring mixer. This mixer, shown in Fig. 1, can be analyzed using a univariate power series to describe the current–voltage characteristics of each diode, but this method requires the use of iterative techniques to satisfy Kirchhoff's voltage and current laws for the circuit [4]. The behavioral model presented here can be used as a voltage-controlled voltage source in a GPSA simulator such as FREDA [4] or in a block system simulator such as CAPSIM [5].

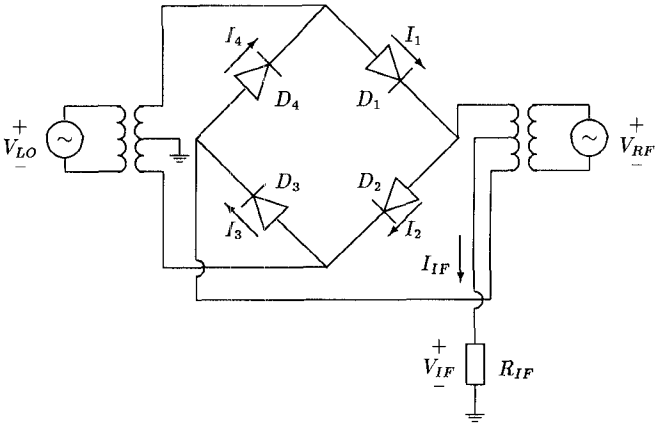

Fig. 1. Diode ring mixer.

II. Development of Algebraic Formulas

In this section we derive an algebraic formula for the output components of a nonlinearity which can be described by a power series in two variables having complex coefficients and frequency-dependent time delays when the inputs are sums of sinusoids.

A nonlinear element or system having the two multifrequency inputs $x(t)$ and $z(t)$ (each having N components),

$$x(t) = \sum_{k=1}^{N} x_k(t) = \sum_{k=1}^{N} |X_k| \cos(\omega_k t + \phi_k) \tag{1}$$

and

$$z(t) = \sum_{k=1}^{N} z_k(t) = \sum_{k=1}^{N} |Z_k| \cos(\omega_k t + \theta_k) \tag{2}$$

can be represented by the bivariate generalized power series

$$y(t) = \sum_{\sigma=0}^{\infty} \sum_{\rho=0}^{\infty} a_{\sigma,\rho} f(\sigma, x) g(\rho, z) \tag{3}$$

with

$$f(\sigma, x) = \left(\sum_{k=1}^{N} b_k x_k(t - \tau_{k,\sigma}) \right)^{\sigma} \tag{4}$$

and

$$g(\rho, z) = \left(\sum_{k=1}^{N} d_k z_k(t - \lambda_{k,\rho}) \right)^{\rho}. \tag{5}$$

In these expressions, $a_{\sigma,\rho}$ is a complex coefficient, b_k and d_k are real, and $\tau_{k,\sigma}$ and $\lambda_{k,\rho}$ are time delays that depend on both the order of the power series and the index of the input frequency components. Our aim is to rewrite (3) in terms of phasors. The x input can be expressed as

$$\begin{aligned} x_k(t - \tau_{k,\sigma}) &= |X_k| \cos(\omega_k t + \phi_k - \omega_k \tau_{k,\sigma}) \\ &= \frac{1}{2} X_k \Gamma_{k,\sigma} e^{j\omega_k t} + \frac{1}{2} X_k^* \Gamma_{k,\sigma}^* e^{-j\omega_k t} \end{aligned} \tag{6}$$

Manuscript received October 2, 1989; revised January 17, 1990. This work was supported by an NSF Presidential Young Investigator Award (ECS-8657836) to M. B. Steer and by IBM.

P. J. Lunsford II is with IBM, mailstop D63/061, P.O. Box 12195, Research Triangle Park, NC 27709.
G. W. Rhyne was with the Department of Electrical and Computer Engineering, North Carolina State University, Raleigh, NC 27695. He is now with Motorola Corporate Research Laboratories, 2100 East Elliot Rd., Tempe, AZ 85284.
M. B. Steer is with the Department of Electrical and Computer Engineering, North Carolina State University, Raleigh, NC 27695-7911.

IEEE Log Number 9034848.